Multi-Channel Cascadable Parametric Signal Processing for Wavelength Conversion and Nonlinearity Compensation

Shu Namiki, *Senior Member, IEEE, Fellow, OSA*, Karen Solis-Trapala, *Member, IEEE*, Hung Nguyen Tan, *Member, IEEE, Member, OSA*, Mark Pelusi, *Senior Member, IEEE, Senior Member, OSA*, and Takashi Inoue, *Member, IEEE*

(Invited Paper)

***Abstract*—The dissemination of the digital coherent technology has enabled the recent growth of information networks, which has obviated signal processing in the optical domain such as optical dispersion compensation. However, the further scaling of the digital coherent technology will eventually suffer from the slowdown of the Moore's law and/or the energy crunch as a result of the longstanding relentless traffic increase. The use of all-optical signal processing, free from the electronic limitations, will then inevitably be reevaluated but in a slightly different way from how it was previously expected. In this paper, we highlight the unique features of all-optical signal processing that outperforms digital signal processing, and review the two latest results: one is upgrade-free, multi-channel wavelength conversion; and the other, all-optical back propagation for WDM channel nonlinearity compensation. Both of these functions are exploiting a versatile physical phenomenon of parametric processes in highly nonlinear fiber that is highly efficient in terms of cost and energy and is as cascadable as EDFAs. This paper discusses their practical aspects with emphasis on cascadability. In particular, the promising prospects for "cascaded phase-conjugating amplifier chains" to compensate nonlinear signal distortion will be highlighted after discussing the parameter tolerances for all-channel nonlinearity compensation.**

***Index Terms*—Fiber nonlinearity, highly nonlinear fiber, optical fiber networks, optical phase conjugation, optical signal processing, optical wavelength conversion.**

Manuscript received May 29, 2016; revised August 18, 2016; accepted August 25, 2016. Date of publication August 29, 2016; date of current version February 22, 2017. This work was supported in part by the Project for Developing Innovation Systems of the MEXT, Japan.

S. Namiki and T. Inoue are with the National Institute of Advanced Industrial Science and Technology, Tsukuba 305-8568, Japan (e-mail: shu.namiki@aist.go.jp; inoue.takashi@aist.go.jp).

K. Solis-Trapala was with the National Institute of Advanced Industrial Science and Technology, Tsukuba 305-8568, Japan, when she contributed to this paper, and currently with EFFECT Photonics, Eindhoven 5617BC, The Netherlands (e-mail: karensolis@effectphotonics.nl).

H. Nguyen Tan was with the National Institute of Advanced Industrial Science and Technology, Tsukuba 305-8568, Japan, when he contributed to this paper, and currently with Danang University of Science and Technology. Danang 550000, Vietnam (e-mail: hung.nguyen@dut.udn.vn).

M. Pelusi is with the Centre for Ultrahigh Bandwidth Devices for Optical Systems, Institute of Photonics and Optical Science, School of Physics, University of Sydney, Sydney, N.S.W. 2006, Australia (e-mail: m.pelusi@physics.usyd.edu.au).

Color versions of one or more of the figures in this paper are available online at http://ieeexplore.ieee.org.

Digital Object Identifier 10.1109/JLT.2016.2604386

I. Introduction

THE dramatically increasing information traffic on the Internet will finally reach the point at which the energy consumption begins to severely limit the capacity of the overall network [1]. This phenomenon will be observed not only in the wide area networks but also in mega-datacenters, where the aggregate bandwidth of the leaf-spine switch fabric has exceeded 1 Pb/s [2] and is extrapolated to increase beyond 1 Eb/s circa 2030. It is easily generalized from these cases that the switch will be the ultimate bottleneck of the network everywhere.

Replacing power-hungry electrical switches, such as routers, with optical path switches is challenging but is the only means to substantially resolve the energy crunch of the network [3]. Migration from the current network to a network based on optical path switches could only be realized through introducing a new network framework like software defined networking. In other words, optical path switching necessitates a centralized control plane that is separated from data plane. The network comprising optical path nodes controlled by a resource management is called "Dynamic Optical Path Network (DOPN)" [4]. The scalability of DOPN is primarily limited by the port count of optical switches. In order to overcome this limitation and achieve nationwide scalability, hierarchical multi-granular path structure is introduced [5], where Flex-grid "colorless, directionless and contentionless" (CDC)-ROADM (viz. CDC(G)-ROADM) technology [6], as well as fiber matrix switches and optical data unit cross-connects, plays an important role. On the other hand, the metro area network based on ROADM rings is growing to be a greater mesh network by introducing CDC(G)-ROADM technology [7].

In the process of migrating from conventional ROADM ring networks to full-mesh DOPN, two major challenges are faced in the physical layer. One is the limited wavelength resources and the other is the Shannon-limited reachability of signals with advanced modulation formats [8]. This paper addresses that both of these issues could be better resolved by means of multi-channel cascadable parametric signal processing based on highly nonlinear fiber (HNLF), rather than by electronic means [9].

To mitigate the former problem, efficient tunable wavelength converters (WCs) will be a key. In a CDC(G)-ROADM based

mesh network, a single wavelength must be assigned to one fiber link that spans across many ROADM nodes, and the same wavelength cannot be assigned to two or more optical paths on a fiber, which is the cause of spectral fragmentation and lowers the overall network utilization. To mitigate spectral fragmentations and improve the network utilization, introducing tunable WCs has been shown to be attractive and effective [9]–[12]. In this context, the method of wavelength conversion does not matter. However, in the following sections, we will discuss the compelling advantages of all optical WCs over the opto-electronic equivalent.

The latter issue is how we can mitigate nonlinearities in order to overcome the nonlinear Shannon limit. Due to the optically switched paths, signals will tend to stay in the optical domain longer than in conventional networks. While there have been extensive research activities on all-optical regeneration and tunable dispersion compensation for the realization of DOPN [13], rapid advancement of digital coherent and forward error correction technologies have obviated many all-optical signal processing techniques to cure signal impairments. As a consequence, nonlinear distortions have remained as the ultimate signal impairment. To tackle this, the digital signal processing (DSP) method of digital back propagation (DBP) was employed [14]. In fact, the computation power required to fully perform the DBP of high-capacity WDM transmission is far beyond the capability of the present DSP technology, and thus a practical implementation of DBP must be compromised with a coarsely approximated single-channel treatment [15]. For the future scaling of DSP or computing in general beyond the end of Moore's law, extensive research efforts are being made to pursue breakthroughs at a level of more fundamental physics: e.g., replacing more standard DSP by completely new processes directly exploiting physical phenomena, such as quantum annealing [16] and optical Ising machines [17]. All-optical nonlinearity compensation using optical phase conjugation (OPC) may be analogous to such ground-breaking approaches, and has been studied in this context [9], [18]–[21].

The structure of this paper is as follows: Section II summarizes the key features of parametric signal processing using the state-of-the-art HNLF, finding wavelength conversion and OPC based nonlinearity compensation as its compelling applications. Section III then refers to the utility of all-optical WCs with respect to their opto-electronic counter-part. Section IV develops the technology of all-optical nonlinearity compensation based on multi-channel OPC. Section V further discusses plausible practical implementations of all-optical nonlinearity compensation. Section VI concludes the paper.

II. Features of Parametric Signal Processing

The key features of four wave mixing (FWM) in HNLF for enabling WC and OPC functions have been discussed in [13]. In summary, the features are:

1) Low loss and low noise (for cascadability);
2) wide (seamless and gridless) band;
3) full tunability over C- and/or L-band;
4) channel count, modulation format, and bitrate agnostic operations;
5) ultrafast response free from transients;
6) low cost and small footprint;
7) high reliability.

The reason for the features 6) and 7) is because the basic configuration of parametric devices based on HNLF is closely analogous with EDFAs. In general, they consist of an optical transmission fiber, pump-signal combiners, isolators, single-frequency tunable lasers with EDFAs for pumps, tunable filters, phase modulator if pump dithering is necessary, and so on. Among these, only the tunable filters may not be off-the-shelf yet. With these features, plausible applications based on parametric signal processing, include:

1) Parametric amplification including phase sensitive amplifiers (PSA);
2) tunable WC/translator;
3) tunable dispersion and delay compensator;
4) OPC for nonlinearity and dispersion compensation;
5) all optical sampling;
6) optical regenerator, including phase regenerator by PSA;
7) clock recovery, etc.

For cost and energy savings, applications capable of multi-channel operations in a single subsystem are generally more effective than single-channel operations. Considering its impact, this paper focuses upon multi-channel all-optical WCs and all-WDM channel nonlinearity compensation.

TABLE I
Comparison Between All-Optical and Opto-Electronic WCs

	Opto-electronic	Optical
Principle	O/E and E/O Conversions	FWM
Bandwidth	Limited by electronics (<100 GHz)	Wide (>1 THz)
Modulation format, Symbol rate	Fixed by electronics	Agnostic
Number of channels	Single channel	Multiple channels
CAPEX/OPEX	High/High	Low/Very Low
Cascadability	Arbitrary	Almost same as EDFA

III. Multi-Channel All-Optical WCs

While opto-electronic (O/E-E/O) wavelength conversion can be off-the-shelf ready for commercial systems, all-optical wavelength conversion based on FWM in HNLF still has compelling advantages when adopting our proposed "two-stage counter-dithered" degenerate FWM scheme [22]. With this method, we have succeeded in realizing fully telecom-grade operations of wavelength conversion because it allows:

1) Guard band less (even overlapping) operations over the entire operating telecom window such as C-band;
2) not only multiple-wavelength but also modulation-format and bitrate agnostic operations;
3) cascaded operation, as cascadable as EDFAs.

These features thus bring unique merits in terms of cost, both CAPEX and OPEX, and flexibility of the network. The comparison between all-optical and opto-electronic WCs is summarized in Table I.

As a primary assumption made in Table I, heterogeneous multiple signal formats will be used in the same WDM network. Such an environment should be inevitable sooner or later due to

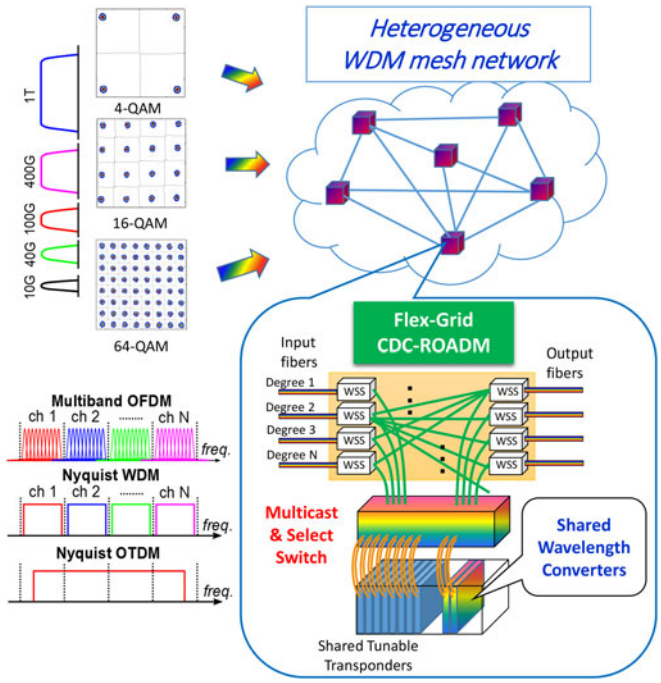

Fig. 1. Heterogeneous WDM network based on flex-grid CDC-ROADM with shared all-optical WCs.

the dissemination of software defined open and disaggregated transport technology [23]. An example of the CDC(G)-ROADM equipped with all-optical WCs, along with the network concept, is shown in Fig. 1. Naturally, CDC(G)-ROADM can allow heterogeneous signal formats. While various kinds of multiple opto-electronic WCs will be needed in accordance with the heterogeneity of the signals, only one kind of all-optical WCs, and fewer number, will be needed because of its universal and multi-channel nature. As technology evolves, opto-electronic WCs will have to be upgraded, whereas all-optical ones can stay the same. Therefore, in the future network, the CAPEX and OPEX for all-optical WCs are promisingly low, especially as the number of channels increases.

For cascadability, opto-electronic WCs outperform all-optical ones. However, by increasing the conversion efficiency of the FWM process, we have achieved a noise figure (NF) as low as 6.2 dB, which means that it is almost as cascadable as EDFAs [22]. Fig. 2 shows experimental results of the cascadability of all-optical WCs for 96-Gb/s dual polarization (DP)-16 quadrature amplitude modulation (QAM) signals. The experiment employed a wavelength-translating re-circulating fiber loop scheme in which the number of WDM channels corresponds to the number of loop circulations (see Fig. 2(a)). In the figure, we had ten WDM channels meaning that the input signal went through a cascade of ten all-optical WCs. The Q-factor was plotted against the number of loop, which verifies decent cascadability, despite the relatively poor noise performance of the WC used in the experiment (see Fig. 2(b)). Constellation diagrams of the signals after ten cascaded wavelength conversions are plotted in Fig. 2(c). If all the necessary equipment was used to achieve a NF of 6.2 dB for the loop experiment, the cascadability could have exceeded 20. The detailed analyses of the cascadability of the all-optical WCs are reported in [22].

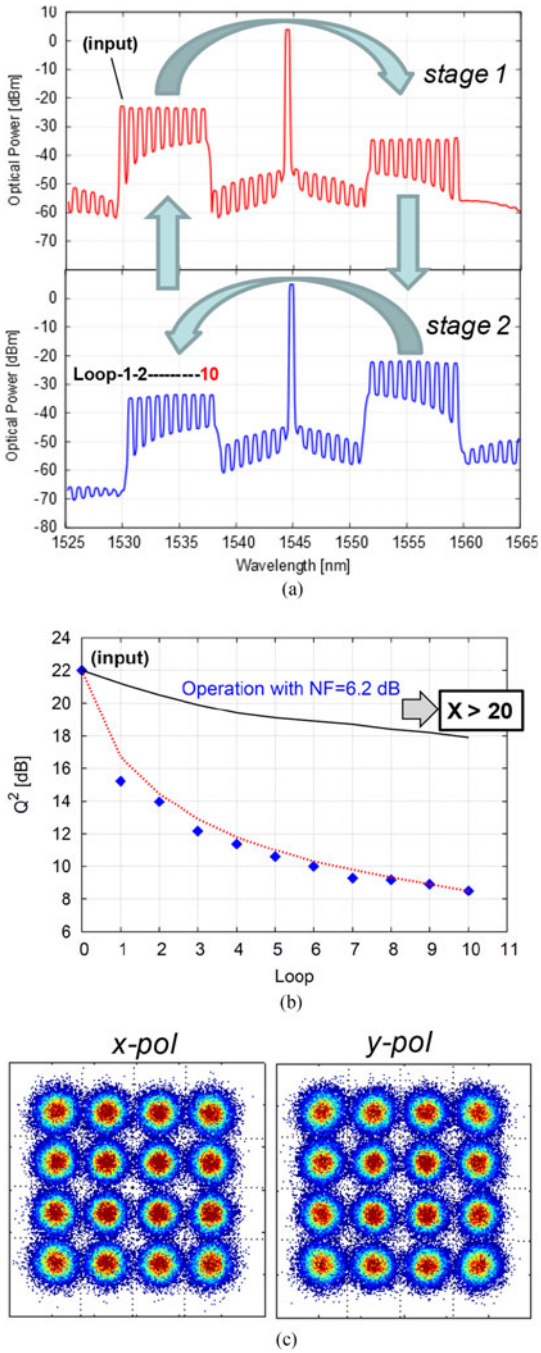

Fig. 2. Results of a cascadability experiment for all-optical WCs using a wavelength-translating loop for 96-Gb/s DP-16QAM signals: (a) Optical spectra of the signals circulating inside the wavelength-translating loop; (b) Q-factor versus the number of loops. Diamonds are the experimental results. Dashed and solid lines are theoretical predictions for the experiment and the case with a NF of 6.2 dB; (c) constellation diagrams of the signals after ten loops.

IV. All-Optical Nonlinearity Compensation Through Multi-Channel OPC

A. Principle

The proposition of the principle of the OPC-based nonlinearity compensation dates back to the 70's [24], and was followed by experimental demonstrations for optical fiber

communications in the 90's [25]. In all-optical nonlinearity compensation using FWM based parametric process, the signals remain in the optical domain, unlike for DSP-DBP, and are physically phase-conjugated halfway by FWM in HNLF, and transmitted over the latter half of the fiber span. Namely, the latter half transmission needs to be designed so as to be the virtual back propagation of the first half [26]. In this sense, this process can be regarded as a highly efficient, speed-of-light computation of massive back propagation.

Let us elucidate these processes by looking at the nonlinear Schrödinger equations (NLSE). First, the NLSE is written in general as

$$\frac{\partial A}{\partial z} = -\frac{\alpha}{2}A - \frac{i}{2}\beta_2\frac{\partial^2 A}{\partial t^2} + \frac{1}{6}\beta_3\frac{\partial^3 A}{\partial t^3} + i\gamma|A|^2 A \quad (1)$$

where A is the electric field amplitude as a function of time, t, and propagation distance z, α is the attenuation coefficient of the fiber, β_2 and β_3 are the group velocity dispersion (GVD), and third-order dispersion (TOD), respectively, and γ is the nonlinear coefficient. Propagation of the optical signals over the first half span is given by integrating Eq. (1) from the transmitter to the halfway point while its back propagation is given by its reverse integration. This can be expressed by changing the sign of the right hand side of Eq. (1), i.e.,

$$\frac{\partial A}{\partial z} = +\frac{\alpha}{2}A + \frac{i}{2}\beta_2\frac{\partial^2 A}{\partial t^2} - \frac{1}{6}\beta_3\frac{\partial^3 A}{\partial t^3} - i\gamma|A|^2 A. \quad (2)$$

Equation (2) corresponds to the time reversal of Eq. (1), which is unphysical and can only be solved in the digital domain. Of course, digital solving of Eq. (2) for long haul massive dense WDM signals is non-trivial and consumes huge amount of computation resources that may not be fit in a gold box of a transceiver. On the other hand, instead of computing the time reversal, spectral inversion can be done in the optical domain by parametric processes. After the mid-span phase conjugation, the phase-conjugated optical signals will obey the following equation:

$$\frac{\partial A^*}{\partial z} = -\frac{\alpha}{2}A^* + \frac{i}{2}\beta_2\frac{\partial^2 A^*}{\partial t^2} + \frac{1}{6}\beta_3\frac{\partial^3 A^*}{\partial t^3} - i\gamma|A|^2 A^*. \quad (3)$$

By comparing Eq. (3) with Eq. (2), one can imagine that all the terms on the right hand side can be identical if α and β_3 in Eq. (3) have the same absolute magnitudes with the opposite sign as those in Eq. (2), respectively. Of course, the physical propagation occurs from the halfway point to the receiver, the latter half of the transmission span has to have the physical properties correspondingly determined by those of the first half span such that

$$\begin{aligned} \alpha^{(2)}(z) &= -\alpha^{(1)}(L - z), \\ \beta_2^{(2)}(z) &= \beta_2^{(1)}(L - z), \\ \beta_3^{(2)}(z) &= -\beta_3^{(1)}(L - z), \\ \gamma^{(2)}(z) &= \gamma^{(1)}(L - z), \end{aligned} \quad (4)$$

where superscripts (1) and (2) indicate the first and second span, respectively, and L is the total distance assuming the OPC is located at $z = L/2$. Whereas the nonlinear coefficient can be regarded as constant in most cases, the dispersion and power excursion profiles have to be designed so as to be mirror symmetric with respect to the halfway point ($z = L/2$) in order to completely cancel loss, GVD, TOD, and Kerr nonlinearities. Any failure in meeting these conditions results in un-cancelled portions of signal distortion.

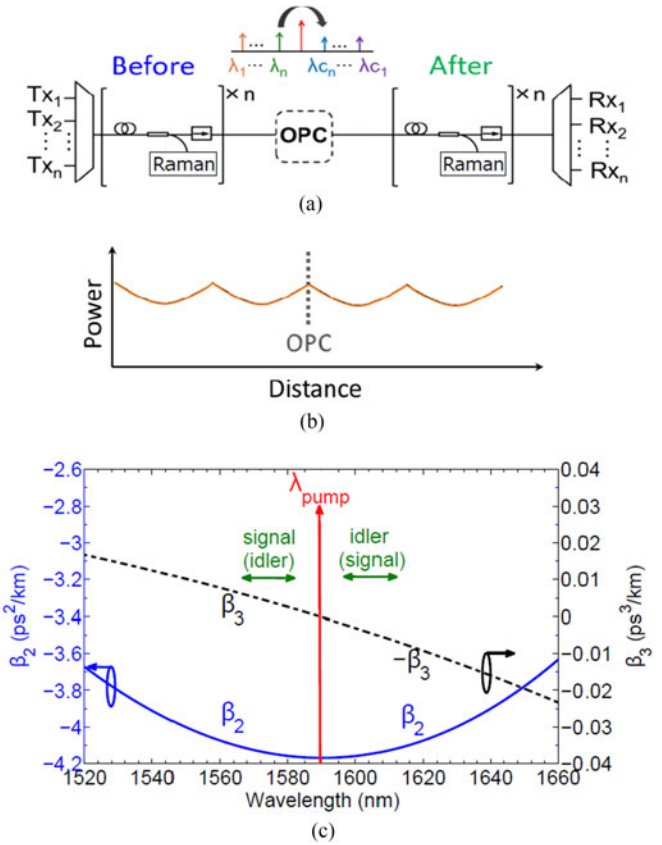

Fig. 3. Proposed scheme for complete nonlinearity compensation. (a) The transmission line, (b) symmetric power excursion profile by means of backward-pumped distributed Raman amplification, (c) symmetric dispersion profile of actually developed fiber [28].

B. Proof-of-Concept Experiment

In order to realize conditions (4), we employed distributed Raman amplification and a pair of fibers with opposite TODs, as previously proposed to be feasible. The details are illustrated in Fig. 3 and reported in [26] and [27]. As shown in Fig. 3(a), OPC is positioned halfway along the transmission line. Backward-pumped distributed Raman amplifiers (DRA) are capable of realizing a symmetric profile of the signal power excursion versus distance with respect to the OPC position as depicted in Fig. 3(b). A dispersion flattened fiber has been developed to realize a symmetric dispersion profile [28], at a specific center wavelength obtained by optimally locating the CW pump to satisfy all the conditions in Eq. (4), as delineated in Fig. 3(c). In this scheme, the first half of the transmission is assumed to be in the C-band while the second half is in the L-band, or vice versa.

A preliminary experiment with 24-km fiber span produced a 10-dB improvement in the nonlinear threshold power where

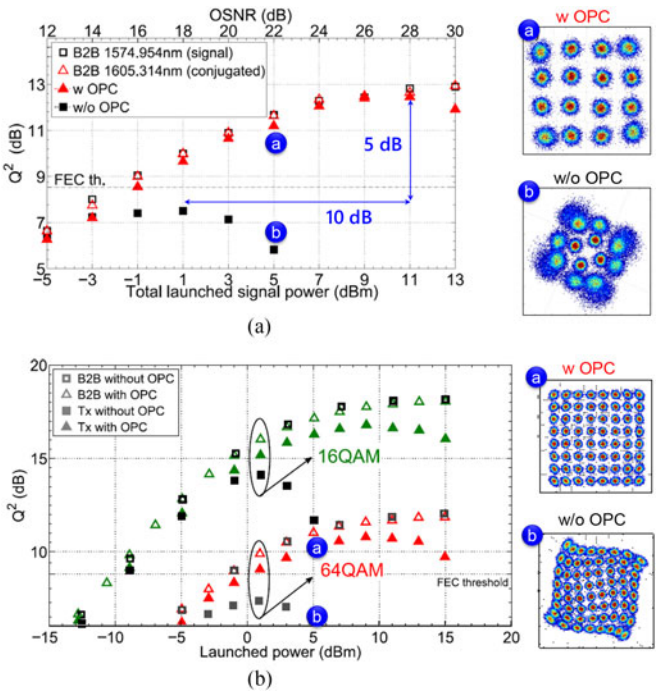

Fig. 4. Q^2 factor as a function of total launched signal power and OSNR for (a) a 24 km long 4 × 12-Gbaud 16-QAM WDM transmission [27], and (b) single-channel 12-Gbaud 16- and 64-QAM signals.

the maximum Q-factor is reached, as shown in Fig. 4. Numerical studies also showed ∼10 dB improvement in the nonlinear threshold for 67.25 Gbaud WDM 2000-km transmission [27]. We have also succeeded in achieving about 8 dB improvement in single-channel 12-Gbaud 16- and 64-QAM signals. Fig. 4(a) and simulations at 67.25 GBaud corresponded to setting the pump at an optimum wavelength in the L-band, while the experiment in Fig. 4(b) corresponded to the pump in the C-band, i.e., one may attribute the difference in nonlinear threshold improvement to a residual dispersion asymmetry in the C-band case. In simulations with standard single mode fiber (SSMF), it was confirmed that the dispersion imbalance was noticeable at distances as short as 24 km. In either case, the values are significantly better than for any DBP approach that usually obtain only around 1-2 dB improvement [15].

V. Towards Practical Implementations

In this section, we discuss the parameter tolerances of all-optical nonlinearity compensation, and the promising prospects of our proposed "phase-conjugating amplifier chain" for practical implementation.

A. Parameter Tolerances

To roughly grasp the parameter tolerances of our scheme, we conducted simulations employing a commercial tool (Optisystem 11). Based on the scheme of Fig. 3, we varied the degree of symmetry in terms of signal power excursion and GVD. We also estimated the impact of fiber birefringence from polarization mode dispersion (PMD).

We considered the transmission of 4 × 269 Gb/s 16QAM WDM channels (ranging from 1573.301 to 1575.782 nm) with a 100 GHz spacing and combined by a multiplexer with a 80.7 GHz third order Gaussian passband. The optical transmitter was based on the superposition of two QPSK signals, one of which has a 6dB attenuated output. A total of 2^{10} symbols per channel were transmitted with 256 samples/symbol. The transmission line consisted of $N \times 50$ km spans of NZDSF (Chromatic dispersion $D = 3.13$ ps $\cdot$ nm^{-1} $\cdot$ km^{-1}, dispersion slope $S = 0.0032$ ps $\cdot$ nm^{-2} $\cdot$ km^{-1} loss $\alpha = 0.227$ dB/km, effective area $A_{\text{eff}} = 41.4$ μm^2). Distributed Raman amplification was used to compensate for the losses along the system. A backward propagating, five wavelength pumping scheme [29] was designed to provide a net 0 dB flat gain (less than 0.5-dB gain ripple) to the signals with a highly symmetric power profile, as shown later. At the receiver, the signals were demultiplexed (with 80.7 GHz third order Gaussian passband), then preamplified (to constant power of 0 dBm) and fed into a 90° hybrid connected to four balanced photodiodes. The I and Q output signals were then processed by an electrical constellation analyzer to quantify the Q factor. The photodiodes responsivity and dark current were set to 0.5 A/W and 5 nA, respectively. Thermal noise and shot noise were neglected in the simulation. The local oscillator wavelength coincided with the received channel. Because we were interested in assessing the improvement offered by the nonlinearity compensation scheme, the effects of laser linewidth and PMD were neglected, unless otherwise specified.

The OPC subsystem was based on a 100-m long HNLF with zero-dispersion wavelength $\lambda_0 = 1590.2$ nm, nonlinear coefficient $\gamma = 14$ W^{-1} $\cdot$ km^{-1}, $\alpha = 1.53$ dB/km and $S = 0.0075$ ps $\cdot$ nm^{-2}$\cdot$km^{-1}. A 28 dBm CW pump located at 1589.989 nm produced a FWM power conversion efficiency of -3.5 dB, resulting in only a marginal penalty (0.8 dB). It should be noted that the effect of stimulated Brillouin scattering (SBS) was ignored throughout the simulation in order to simplify the discussion. Of course, the suppression of SBS is an important issue for practical implementations of OPC (see, e.g., Ref. [30]).

To test the Q factor penalty tolerance to signal power asymmetry, we fixed the total launched power to the transmission fiber to 7 dBm, which proved to be in the nonlinear transmission regime for a 4 × 67.25 Gbaud-16QAM WDM signal over 2000 km [26]. Signal transmission was investigated for links of varied span length and power profiles, and subsequently, varied path average powers (P_{ave}). Each link consisted of spans of length L_s each with backward propagating, five wavelength Raman pumping, designed to provide a 0 dB net flat gain, but exhibiting different amounts of asymmetry which we characterized as the percentage $\varsigma_s = (L_s P_{\text{ave}})^{-1} \int_0^{L_s} |p(z) - p(L_s - z)| dz \times 100$, where $p(z)$ is a function describing the power excursion in the span. These power profiles are shown in Fig. 5(a), where the associated per span is also indicated. Then, the Q^2 factor penalty (reference being a lossless medium) as a function of ς_s was evaluated as in Fig. 5(b). The results represent the upper limit of the system performance since noise was not included in the simulation; this also allowed focusing on the asymmetry

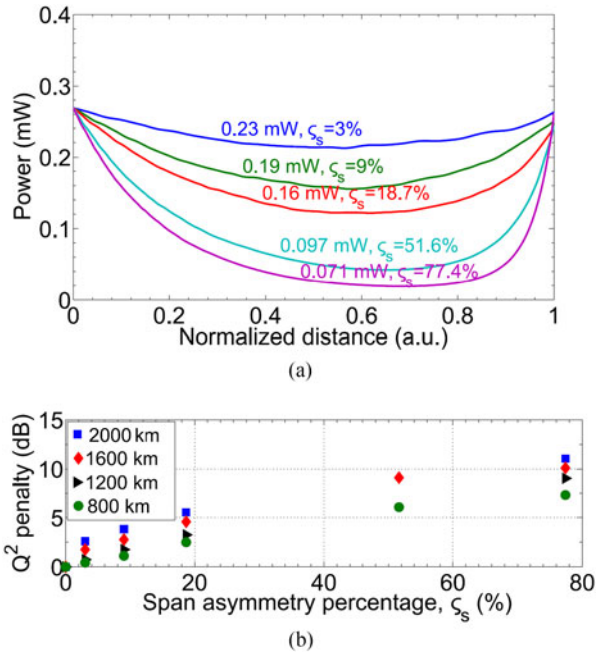

Fig. 5. Impact of signal power asymmetry on an OPC based nonlinearity compensation system with varying transmissions lengths [27]. (a) Power profiles by DRA characterized by P_{ave} and ς_s to test the signal power asymmetry tolerance. (b) Q^2 factor penalty versus ς_s.

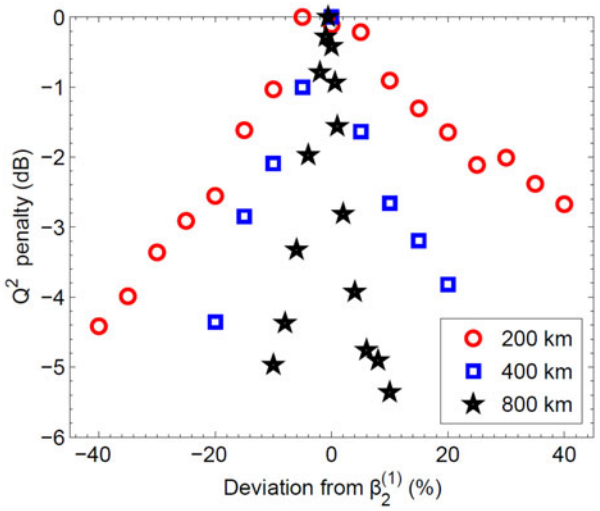

Fig. 6. Q^2 factor impact of GVD deviation from ideal symmetry on an OPC based nonlinearity compensation system with varied transmissions lengths.

quality alone. We note that less than 9% span asymmetries can be achieved for long spans (>50 km) with higher order Raman pumping scheme considered. We refer to [27] for further details on the signal power asymmetry tolerance assessment.

We then investigated the tolerance to the dispersion imbalance by varying the dispersion parameter β_2 of the second part of the link, $\beta_2^{(2)}$(i.e., after OPC) with respect to the dispersion parameter in the first part of the link, labeled as $\beta_2^{(1)}$, while keeping the TOD parameters under ideal conditions, i.e., $\beta_3^{(1)} = -\beta_3^{(2)}$. Fig. 6 shows how severely the tolerance to the dispersion imbalance was reduced as the transmission reach increased. At

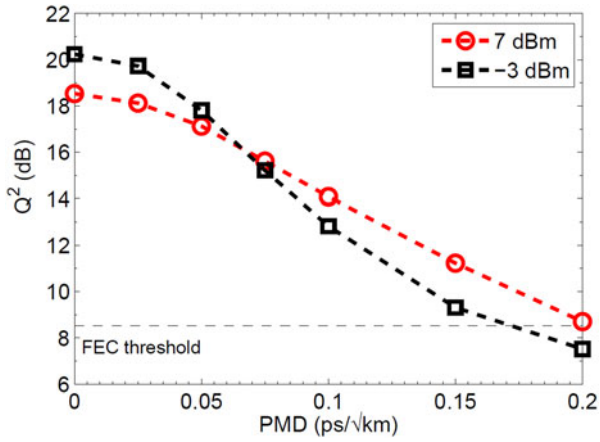

Fig. 7. Impact of birefringence on Q^2 factor for 800-km long nonlinearity compensation transmission system.

800 km, the dispersion tolerance for 2-dB Q^2-factor penalty is reduced to only a few percent. We note that in principle this imbalance can be offset by optimizing the OPC position and input span launch powers.

To roughly estimate the effect of birefringence on the transmission system, we considered a lossless and noiseless 800-km long transmission link. In the simulation tool, birefringence was modeled stochastically, in accordance with the ITU-T G.691 PMD model, by representing the fiber as a concatenation of birefringent trunks of random lengths that follow a Gaussian distribution with average L_{ave} and standard deviation σ. Furthermore there is a random orientation of the principal axes of the trunks with respect to each other for which PMD is defined. Using $L_{\text{ave}} = 200$ m and $\sigma = 40$ m, we evaluated the Q^2 factor of one of the inner channels for four random state of polarizations (SOPs) of the transmitted channels. The averaged results are shown in Fig. 7 for two launched powers of -3 and 7 dBm, corresponding to a linear and a nonlinear case, respectively.

It is observed that the transmission reach at 800 km is limited by PMD values closer to 0.2 ps/$\sqrt{\text{km}}$. This estimation should yet be taken cautiously as the tests were only performed for four sets of input SOPs, which is perhaps not enough to fully represent the ensembles. Nevertheless, the following consideration can support this estimate. Fig. 7 suggests that the signals after 800-km transmission remain correlated for the PMD below 0.05 ps/$\sqrt{\text{km}}$. Assuming that de-correlation occurs due to walk off, then the average differential group delay (DGD) should be kept much shorter than the symbol length, to within <10% for small Q-factor degradation, considering its Maxwellian nature. In the case of Fig. 7, the symbol length is ∼15 ps. For a fiber with a PMD of 0.05 ps/$\sqrt{\text{km}}$, the expected DGD for an 800-km link is:

$$0.05 \text{ ps}/\sqrt{\text{km}} \times \sqrt{800 \text{ km}} \sim 1.4 \text{ ps}. \quad (5)$$

This value is comparable with 1/10 of the symbol length (1.5 ps), and therefore is consistent with Fig. 7.

According to ITU-T G.652B/D, a PMD of 0.2 ps/$\sqrt{\text{km}}$ is recommended. A PMD of 0.1 ps/$\sqrt{\text{km}}$ is also discussed therein. Although the definition of PMD in this simulation may not be as consistent with that in ITU-T recommendations, it is clear

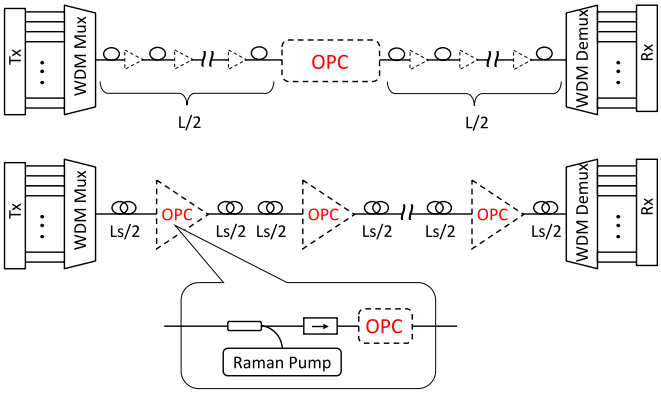

Fig. 8. All-optical nonlinearity compensation scheme: Single OPC scheme (Top); and proposed phase-conjugating amplifier chain scheme (Bottom). L_s is the amplifier spacing.

that the impact of birefringence is non-negligible especially for long haul transmissions. In the following we propose a scheme to suppress the impact of PMD.

B. Phase-Conjugating Amplifier Chain

There are two major drawbacks of the nearly ideal OPC approach described above: one is that we need to deploy a new type of fiber (dispersion flattened fiber); and the other is that we need to prepare the exact symmetry for long haul transmission line including ideally suppressed PMD. Both of these drawbacks can be resolved by introducing "phase-conjugating amplifier chain" as shown in the bottom of Fig. 8. This scheme significantly shortens the span length for which the nonlinearity is compensated. Typical transmission distances for which nonlinearity must be compensated would be from a few hundred to a few thousand kilometers. It would be more difficult to maintain the exact symmetry for longer transmission distances in the single OPC scheme. On the other hand, introducing phase-conjugating amplifiers as shown in the inset of Fig. 8 will make all the parameters more tolerable, even though a number of cascades of phase conjugation are necessary. As amplifier spans are typically between 40 and 100 km, the impact of deviations from the ideal symmetry would be as small. Indeed, shortening the OPC spans has been pointed out as better for suppressing non-deterministic impairments, such as nonlinear interactions with ASE from inline amplifiers [31], signal-ASE (FWM) [32], and the effect from PMD [20], [33], [34]. Besides, even the TOD term could be neglected in the case of SSMF, because in the C-band, the deviation of GVD is only up to 10%. A PMD of 0.1–0.2 ps/$\sqrt{\text{km}}$ would provide a preferable condition for NLC, because the NLC length in this case is ten times shorter than the case of Fig. 7.

To verify the cascade operations of OPCs, we conducted a wavelength translating loop experiment similar to that in Fig. 2 but with propagation through the dispersion flattened fiber described in Fig. 3. Whereas the details have been reported in [19], let us briefly review the results here. Fig. 9 shows the block diagram of the wavelength translating loop for testing the phase-conjugating amplifier chain. Fig. 10 shows the results for 4×48 Gb/s DP-QPSK signals after six circulations of the loop,

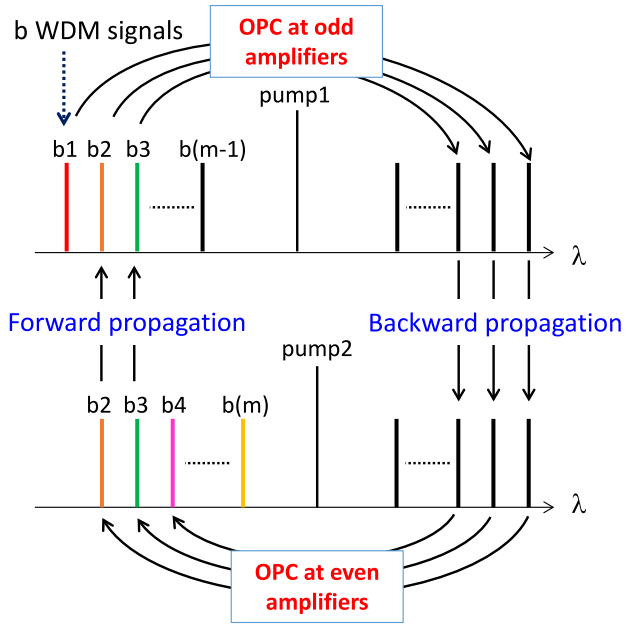

Fig. 9. Schematic diagram of wavelength translating loop experiment for testing the phase-conjugating amplifier chain [19].

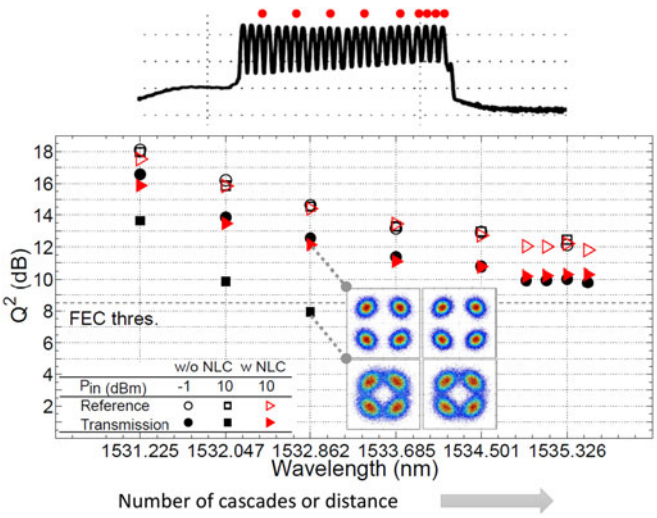

Fig. 10. Experimental results of cascaded operations of all-optical nonlinearity compensation based on wavelength-translating loop [19]. The output optical spectrum from the wavelength-translating loop (top) where the red dots correspond to the plots in the Q^2 factor versus wavelength (bottom). The signal wavelengths shift from shorter to longer wavelengths, corresponding to the number of cascades.

meaning 12 cascaded OPCs. It is conjectured that the evolution of SOPs of all the 24 WDM channels co-propagating in the loop must be considerably randomized due to the birefringence of the loop. Nonetheless, a nonlinear threshold improvement of 8 dB was observed and the transmission reach was significantly extended [19]. It is also noteworthy that a remarkable compensation of fiber nonlinearities was also demonstrated using repeated OPC in a 2.048-Tb/s WDM system with eight 32-Gbaud PDM 16-QAM channels in 900-km SSMF transmission, showing $\sim$10 dB improvement in nonlinear threshold [21].

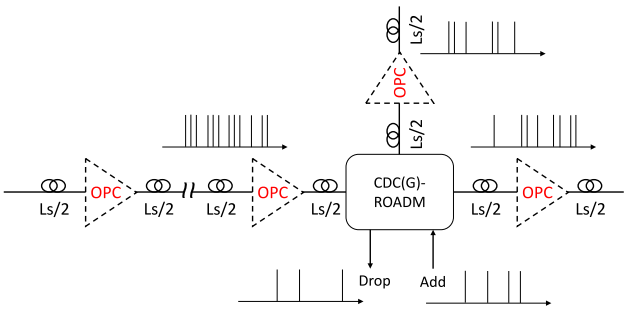

Fig. 11. CDC(G)-ROADM node in a WDM mesh network equipped with phase-conjugating amplifier chain for nonlinearity compensation.

Another merit to introduce the phase-conjugating amplifier chain is the compatibility with WDM networks based on CDC(G)-ROADM. Fig. 11 shows a schematic of CDC(G)-ROADM node in a WDM mesh network equipped with a phase-conjugating amplifier chain for nonlinearity compensation. As can be perceived from the figure, arbitrary exchange and add/drop of WDM channels at the ROADM node do not affect the operations of nonlinearity compensation that are completed within the amplifier spans, while the system has to manage the state of phase conjugation for each signal. In fact, the wavelength-translating loop shown in Fig. 9 can be regarded as repeated "wavelength add" operations of ROADM. Finally, it should be noted that the impact of the randomness of amplifier span lengths has yet to be studied, whereas it may not be as severe as that for a single OPC scheme because the length for nonlinearity compensation is much shorter.

VI. Conclusion

The two important all-optical functions enabled by multi-channel cascadable parametric signal processing, compelling electric approaches, have been highlighted: all-optical multi-channel tunable wavelength conversion; and all-channel nonlinearity compensation using multi-channel OPC. We have shown that more than 20 cascades of all-optical wavelength conversion are feasible for high order modulation formats such as DP-16QAM. After brief explanation of the operating principle, it has been shown that our proposed scheme of all-optical nonlinearity compensation using OPC is capable of achieving a nonlinear threshold improvement of 10 dB. Then, through the numerical studies on its parameter tolerances it was suggested to adopt short and cascaded OPC spans for better and practical nonlinearity compensation. A wavelength-translating loop experiment was then conducted to demonstrate the effectiveness of the phase-conjugating amplifier chain thanks to the cascadability of parametric processes. Realization of all-optical multi-channel wavelength conversion and all-channel nonlinearity compensation based on phase-conjugating amplifier chain will contribute to long term scalability of networks beyond the Moore's law with significant savings of both cost and energy. Finally, we note that our scheme can be most cost-effective for fully loaded WDM systems. Phase-conjugating amplifier chains for fully loaded WDM systems have yet to be experimentally demonstrated.

Acknowledgment

The authors would like to thank Kiyo Ishii for fruitful discussions on optical node architecture, and Trimatiz, Ltd., and Furukawa Electric, Co., Ltd. for their continuous support and collaboration work to develop the wavelength converter and optical phase conjugator using highly nonlinear fiber. M. Pelusi would like to thanks the Australian Academy of Science for supporting his research travel visit.

References

[1] K. Ishii, J. Kurumida, K. Sato, T. Kudoh, and S. Namiki, "Unifying top-down and bottom-up approaches to evaluate network energy consumption" *J. Lightw. Technol.*, vol. 33, no. 21, pp. 4395–4405, Nov. 2015.

[2] A. Singh *et al.*, "Jupiter rising: A decade of clos topologies and centralized control in Google's datacenter network," in *Proc. 2015 ACM Conf. Spec. Interest Group Data Commun.*, pp. 183—197, doi: 10.1145/2785956.2787508.

[3] S. Namiki *et al.*, "Ultrahigh-definition video transmission and extremely green optical networks for future," *IEEE J. Sel. Topics Quantum Electron.*, vol. 17, no. 2, pp. 446–457, Mar./Apr. 2011.

[4] J. Kurumida *et al.*, "First demonstration of ultra-low-energy hierarchical multi-granular optical path network dynamically controlled through NSI-CS for video related applications," presented at the Eur. Conf. Opt. Commun., Cannes, France, 2014, Paper PD 1.3.

[5] K. Ishii, J. Kurumida, S. Namiki, T. Hasama, and H. Ishikawa, "Energy consumption and traffic scaling of dynamic optical path networks," *Proc. SPIE*, vol. 8646, pp. 86460A-1–86460A-10, 2013.

[6] H. Takeshita *et al.*, "Prototype highly integrated 848 transponder aggregator based on si photonics for multi-degree colorless, directionless, contentionless reconfigurable optical add/drop multiplexer," *IEICE Trans. Electron.*, vol. E96-C, no. 7, pp. 966–973, Jul. 2013.

[7] B. Collings, "The Next Generation of ROADM Devices for Evolving Network Applications," presented at the Eur. Conf. Opt. Commun., Geneva, Switzerland, 2011.

[8] R.-J. Essiambre and R. W. Tkach, "Capacity trends and limits of optical communication networks," *Proc. IEEE*, vol. 100, no. 5, pp. 1035–1055, May 2012.

[9] S. Namiki, H. Nguyen Tan, K. Solis-Trapala1, and T. Inoue, "Signal-transparent wavelength conversion and light-speed back propagation through fiber," presented at the Opt. Fiber Commun. Conf., Anaheim, CA, USA, 2016, Paper Th4F.1.

[10] J. M. Simmons, "Analysis of wavelength conversion in all-optical express backbone networks," presented at the Opt. Fiber Commun. Conf., Anaheim, CA, USA, 2002, Paper TuG2.

[11] B. Li and X. Chu, "Routing and wavelength assignment vs. wavelength converter placement in all-optical networks," *IEEE Commun. Mag.*, vol. 41, no. 8, pp. S22–S28, Aug. 2003.

[12] X. Wang, I. Kim, Q. Zhang, P. Palacharla, and T. Ikeuchi, "Efficient all-optical wavelength converter placement and wavelength assignment in optical networks," presented at the Opt. Fiber Commun. Conf., Anaheim, CA, USA, 2016, Paper W2A.52.

[13] S. Namiki, T. Kurosu, K. Tanizawa, S. Petit, M. Gao, and J. Kurumida, "Controlling optical signals through parametric processes," *IEEE J. Sel. Topics Quantum Electron.*, vol. 18, no. 2, pp. 717–725, Mar./Apr. 2012.

[14] E. Ip and M. Kahn, "Compensation of dispersion and nonlinear impairments using digital backpropagation," *J. Lightw. Technol.*, vol. 26, no. 20, pp. 3416–3425, Oct. 2008.

[15] L. Li *et al.*, "Implementation efficient nonlinear equalizer based on correlated digital backpropagation," presented at the Opt. Fiber Commun. Conf., Anaheim, CA, USA, 2011, Paper OWW3.

[16] M. W. Johnson *et al.*, "Quantum annealing with manufactured spins" *Nature*, vol. 473, pp. 194–198, May 2011.

[17] Z. Wang, A. Marandi, K. Wen, R. L. Byer, and Y. Yamamoto, "A coherent ising machine based on degenerate optical parametric oscillators," *Phys. Rev. A*, vol. 88, p. 063853, Nov. 12, 2013.

[18] M. D. Pelusi and B. J. Eggleton, "Optically tunable compensation of nonlinear signal distortion in optical fiber by end-span optical phase conjugation," *Opt. Exp.*, vol. 20, no. 7, pp. 8015–8023, Mar. 2012.

[19] K. Solis-Trapala, M. Pelusi, H. Nguyen Tan, T. Inoue, and S. Namiki, "Optimized WDM transmission impairment mitigation by multiple phase conjugations," *J. Lightw. Technol.*, vol. 34, no. 2, pp. 431–440, Jan. 2016.

[20] A. D. Ellis *et al.*, "4 Tb/s transmission reach enhancement using 10 × 400 Gb/s super-channels and polarization insensitive dual band optical phase conjugation," *J. Lightw. Technol.*, vol. 34, no. 8, pp. 1717–1723, Apr. 2016.
[21] H. Hu, R. M. Jopson, A. H. Gnauck, D. Pilori, S. Randel, and S. Chandrasekhar, "Fiber nonlinearity compensation by repeated phase conjugation in 2.048-Tbit/s WDM transmission of PDM 16-QAM channels," presented at the Opt. Fiber Commun. Conf., Anaheim, CA, USA, 2016, Paper Th4F.3.
[22] H. Nguyen Tan *et al.*, "On the cascadability of all-optical wavelength converter for high-order QAM formats," *J. Lightw. Technol.*, vol. 34, no. 13, pp. 3194–3205, Jan. 2016.
[23] G. Parulkar, T. Tofigh, and M. De Leenheer, "SDN control of packet-over-optical networks," presented at the Optical Fiber Commun. Conf., Los Angeles, CA, USA, 2015, Paper W1G.4.
[24] A. Yariv, D. Fekete, and D. M. Pepper, "Compensation for channel dispersion by nonlinear optical phase conjugation," *Opt. Lett.* vol. 4, no. 2, pp. 52–54, Feb. 1979.
[25] S. Watanabe, T. Chikama, G. Ishikawa, T. Terahara, and H. Kuwahara, "Compensation of pulse shape distortion due to chromatic dispersion and Kerr effect by optical phase conjugation," *IEEE Photon. Technol. Lett.*, vol. 5, no. 10, pp. 1241–1243, Oct. 1993.
[26] K. Solis-Trapala, T. Inoue, and S. Namiki, "Nearly-ideal optical phase conjugation based nonlinear compensation system," presented at the Optical Fiber Commun. Conf., San Francisco, CA, USA, Mar. 2014, Paper W3F.8.
[27] K. Solis-Trapala, T. Inoue, and S. Namiki, "Signal power asymmetry tolerance of an optical phase conjugation-based nonlinear compensation system," presented at the Eur. Conf. Opt. Commun., Cannes, France, 2014, Paper We.2.5.4.
[28] N. Kumano K. Mukasa, S. Matsushita, and T. Yagi, "Zero dispersion-slope NZ-DSF with ultra-wide bandwidth over 300nm," presented at the Eur. Conf. Opt. Commun., Copenhagen, Denmark, 2002, Paper PD1.4.
[29] S. Namiki and Y. Emori, "Ultrabroad-band raman amplifiers pumped and gain-equalized by wavelength-division-multiplexed high-power laser diodes," *IEEE J. Sel. Topics Quantum Electron.*, vol. 7, no. 1, pp. 3–16, Jan./Feb. 2001.
[30] M. Pelusi, K. Solis-Trapala, H. Nguyen Tan, T. Inoue, and S. Namiki, "Multi-tone counter dithering of Tbit/s polarization multiplexed signals for enhanced FWM with a single pump," presented at the Eur. Conf. Opt. Commun., Valencia, Spain, 2015, Paper We.3.6.6.
[31] M. H. Shoreh, "Compensation of nonlinearity impairments in coherent optical OFDM systems using multiple optical phase conjugate modules," *J. Opt. Commun. Netw.*, vol. 6, no. 6, pp. 549–558, Jun. 2014.
[32] A. D. Ellis, M. E. McCarthy, M. A. Z. Al-Khateeb, and S. Sygletos, "Capacity limits of systems employing multiple optical phase conjugators," *Opt. Exp.*, vol. 23, no. 16, pp. 20381–20393, Jul. 2015.
[33] A. D. Ellis, M. A. Z. Al Khateeb, and M. E. McCarthy, "Impact of optical phase conjugation on the nonlinear shannon limit," presented at the Opt. Fiber Commun. Conf., Anaheim, CA, USA, 2016, Paper Th4F.2.
[34] M. E. McCarthy, M. A. Z. Al Kahteeb, F. M. Ferreira, and A. D. Ellis, "PMD tolerant nonlinear compensation using in-line phase conjugation," *Opt. Exp.*, vol. 24, no. 4, pp. 3385–3392, Feb. 2016.

Shu Namiki (M'03–SM'16) received the M.S. degree and the Dr. Sci. degree in applied physics from Waseda University, Tokyo, Japan, in 1988 and 1998, respectively. From 1988 to 2005, he was with Furukawa Electric, Co., Ltd., where he developed award-winning high-power pump lasers and patented multiwavelength-pumped-fiber Raman amplifiers. From 1994 to 1997, he was a Visiting Scientist with Massachusetts Institute of Technology, Cambridge, USA, where he studied mode-locked fiber lasers and ultrashort pulses in fiber. In 2005, he joined the National Institute of Advanced Industrial Science and Technology, Tsukuba, Japan, where he is currently the Director of the Data Photonics Project Unit, and is the Chair of Executive Committee of a national project called "Vertically Integrated Center for Technologies of Optical Routing Toward Ideal Energy Savings (VICTORIES)" in collaboration with ten telecom-related companies. He has authored or coauthored more than 450 conference presentations, papers, book chapters, articles, and patents. He was an Associate Editor and Advisory Editor of the *Journal Optics Express* and the Coeditor-in-Chief of the *IEICE Transactions on Communications*. He was on the Technical Committee for the OFC, the ECOC, the CLEO, the OECC, the OAA, and served as the Program Cochair in the OFC 2015, and will serve as the General Cochair in the OFC 2017. He is a Fellow of the Optical Society of America. He is a Senior Member of the IEEE Photonics Society and Communications Society, and is a Member of the Institute of Electronics, Information, and Communication Engineers, the Japan Society of Applied Physics.

Karen Solis-Trapala (M'11) received the Ph.D. degree in electrical engineering from the Eindhoven University of Technology (TU/e), the Netherlands, in 2011. Her doctoral research focused on the modeling and characterization of quantum-dot based optoelectronic devices with emphasis on microdisk lasers and semiconductor optical amplifiers. After completing her Ph.D. studies, she joined the National Institute of Advanced Industrial Science and Technology (AIST), Japan, where she investigated all-optical regeneration and nonlinearity compensation in optical transmission systems employing advanced modulation formats. Karen enjoys conducting research connecting fundamental device-level physics to system-level developments. She is member of the IEEE Women in Engineering and IEEE Photonics Society.

Hung Nguyen Tan (S'08–M'12) was born in Danang, Vietnam, in 1980. He received the B.E. degree from Danang University of Science and Technology, Danang, in 2003, and the M.E. and Ph.D. degrees from the University of Electro-Communications, Tokyo, Japan, in 2009 and 2012, respectively. From 2012 to 2016, he was a Researcher with the National Institute of Advanced Industrial Science and Technology, Tsukuba, Japan, where his research interests was ultra-fast and spectrally efficient all-optical network technologies, and development of a practical all-optical wavelength converter. He is currently a Teacher in the Department of Electronic and Telecommunication Engineering, The Danang University of Science and Technology. He is a Member of the Optical Society of America and the IEEE Photonics Society.

Mark Pelusi (SM'10) received the Ph.D. degree in electrical engineering from the University of Melbourne, Parkville, Vic., in 1998. He has held research positions as a NEDO Research Fellow with the Femtosecond Technology Research Association, Japan, and Senior Hardware Engineer at Corvis, Corp., USA. In 2014, he was a Visiting Researcher with the National Institute of Advanced Industrial Science and Technology, supported by a travel grant from the Australian Academy of Science. He is currently a Senior Research Fellow and ARC Future Fellow with the School of Physics, University of Sydney, Sydney, N.S.W., Australia. He has authored or coauthored 70 journal papers and 110 conference presentations. His research interests include high-speed photonics and optical signal processing, nonlinear fiber optics, and high bit rate optical fiber communications. He is a Senior Member of the Optical Society of America.

Takashi Inoue (S'00–A'02–M'03) received the Ph.D. degree in communications engineering from Osaka University, Osaka, Japan, in 2002. He joined Furukawa Electric, Co., Ltd., Ichihara, Japan, in 2002, where he studied optical signal processing devices based on nonlinear fiber optics and silica-based planar lightwave circuit. In 2011, he joined the National Institute of Advanced Industrial Science and Technology, Tsukuba, Japan, where he is currently working on digital coherent transmission systems and optical signal processing devices for realizing dynamic optical-path network. He is a Member of the IEEE Photonics Society.